Effect of ionic liquid addition on PVDF – a density functional theory study

Tarun Kumar Kundu, Ranjini Sarkar
Department of Metallurgical and Materials Engineering,
Indian Institute of Technology Kharagpur, Kharagpur, West Bengal, India-721302
tkkundu@metal.iitkgp.ac.in, ranjini_sarkar@iitkgp.ac.in

Keywords: DFT-D, interaction energy, HOMO-LUMO, MEP, NBO, Hirshfeld surface, QTAIM, RDG, NCI

1. Introduction

β-polyvinylidene fluoride (β-PVDF) is one of the most well-known electro-active polymers, which is used in piezoelectric sensors, actuators, and energy storage devices [1]. Direct synthesis of β-PVDF is difficult owing to its unstable all-trans configuration [1, 2]. During synthesis, α-PVDF (with stable trans-gauche configuration) is formed predominantly and then it is converted to β-PVDF using mechanical stretching, electrical poling, and addition of different second phase materials (e.g, ferroelectric ceramic nanoparticles, hydrated salts, metal hydroxides, ionic liquids, etc) [3]. The present study provides detailed quantum chemical description of the molecular interaction between PVDF and 1-n-alkyl-3-methylimidazolium-tetrafluoroborate ([C_nMIM][BF_4] [n = 2,4,6,8,10]) ionic liquids using dispersion corrected density functional theory [4] based on linear combination of atomic orbitals (LCAO) approach [5]. Magnitudes of interaction energy and the dipole moment values of PVDF/IL systems suggest better interaction of ionic liquids with β-PVDF than with α-PVDF. The effect of ionic liquids on the properties of PVDF is found as independent of the length of the alkyl chain present in the IL cation. Therefore, the extent and the positions of weak inter-unit interaction regions are investigated only for β-PVDF/[C4MIM][BF_4] (or [BMIM] [BF_4]) in the terms of natural bond orbital (NBO) analysis [6], Bader's quantum theory of atoms in molecules (QTAIM) [7], Hirshfeld surface plot [8] mapped onto electron density, and reduced density gradient (RDG) analysis and non-covalent interaction (NCI) isosurface plot [9]. Both anion and cation of ionic liquids are found to show weak van der Waals interaction with PVDF molecule but the IL-anion/β-PVDF interaction is found comparatively higher than IL-cation/β-PVDF interaction. Frontier molecular orbital analysis is carried out and different chemical parameters like electronegativity, chemical potential, chemical hardness, softness and electrophilicity index are calculated using Koopmans theorem [10]. Thermochemical calculations [11] are also performed and the variation in different standard thermodynamic parameters with temperature is formulated.

2. Computational details

All the density functional theory calculations are performed using Gaussian 09 [12]. Dispersion corrected exchange correlation density functional B3LYP-D [4] along with 6–311 + G(d, p) [6] basis set are used for geometry optimization and frequency calculations for the systems under study. Gaussview 5.0 [13] is used for visualization of the structures of the molecules, frontier molecular orbitals, and molecular electrostatic potentials mapped onto electron density. NBO analysis is carried out in NBO 3.1 program [12] implemented in Gaussian09. Multi wavefunction analyser (Multiwfn) [14] is used for the analyses of orbital composition, Bader's QTAIM, Hirshfeld surface, and of NBO orbitals plot. Calculations for NCI iso-surface plot are carried out in NCIPLOT-1.0 [9] and visual molecular dynamics (VMD) [15] is used for visualization of Hirsfeld surface, NCI isosurfaces, and RDG plot. Perl code thermo.pl [16] is used to formulate the temperature dependence of the standard thermodynamic parameters. The interaction energy (ΔE) values are calculated using

equation 1 and stabilization energy $E^{(2)}$ is mathematically defined using the second order perturbation theory as given in equation 2.

$$\Delta E = E_{PVDF+IL} - (E_{PVDF} + E_{IL}) \tag{1}$$

where, $E_{PVDF+IL}$ – energy of optimized ionic liquid added β-PVDF molecule, E_{PVDF} – energy of optimized pure β-PVDF molecule and E_{IL} – energy of optimized pure ionic liquid molecule.

$$E^{(2)} = \Delta E_{ij}^{(2)} = \frac{q_i F(i,j)^2}{\varepsilon_j - \varepsilon_i} \tag{2}$$

where, q_i is donor orbital occupancy; ε_i, ε_j are diagonal elements of the Fock matrix; $F(i,j)$ are the off-diagonal elements of the Fock matrix [17].

3. Results

Geometry optimization is performed for four monomer units of pristine α-PVDF chain, β-PVDF chain, [CnMIM][BF_4] (n = 2,4,6,8,10), α-PVDF/[CnMIM][BF_4], and β-PVDF/[CnMIM][BF_4] (n = 2,4,6,8,10). Frequency calculations performed on all the optimized structures obtained zero imaginary frequencies, except for pristine β-PVDF. Three negative frequencies (although low enough to be neglected) ensured the structural instability of all-trans β-PVDF configuration (with CS symmetry) compared to trans-gauche α-PVDF configuration (with C_1 symmetry). Moreover, β-PVDF possesses higher energy and higher dipole moment than α-PVDF (refer Table 1) which is another evidence of instability associated with the former. On the contrary, lower energy and dipole moment values are obtained for β-PVDF/IL than α-PVDF/IL (Table 2). Besides, the interaction energy (ΔE) values of β-PVDF/IL are found as more negative compared to α-PVDF/IL. These facts collectively justify better ion-dipolar interactions in case of β-PVDF/IL and can be correlated to the fact that ionic liquid addition induces formation of β-PVDF crystals from PVDF blend [3]. Notably, ΔE and dipole moment values are found to be independent of the alkyl chain length of IL cation.

Table 1. Properties of isolated α-PVDF and β-PVDF chains.

Properties	α-PVDF with four monomer units	β-PVDF with four monomer units
Zero point energy (a.u)	–1110.026	–1110.012
HOMO-LUMO gap (eV)	8.94	8.21
Dipole moment per monomer unit (C-m)	4.13E-30 {4.00E-30}*	7.28E-30 {7.00E-30}*
Polarizability per monomer unit ($C\text{-}m^2/V$)	4.03E-40 {3.56E-40}*	4.10E-40 {3.63E-40}*
Structure (Point group)	TGTG' (C_1)	TTTT (C_S)

* experimental values are given within {} and taken from [19]

In case of isolated β-PVDF molecule, carbon atoms in the polymer backbone chain and the fluorine atom pairs in β-PVDF molecule share almost equal contribution to the highest occupied molecular orbital (HOMO), and the lowest unoccupied molecular orbital (LUMO) is mainly consisted of C and H atoms. In case of isolated IL and as well as β-PVDF/IL complex molecules, the carbon and the nitrogen atoms present in the imidazolium ring contribute to the highest portion to both the total HOMO and LUMO distribution (Figure 1a). HOMO-LUMO gap for isolated β-PVDF molecule is higher than that of β-PVDF/IL complexes (Table 1 and 2) and these values become almost constant with the variation in alkyl chain length attached to the imidazolium ring. Molecular electrostatic potential plots, mapped onto the electron density values, suggest that, for β-PVDF/IL

complexes, IL-anionic part of the complex [BF_4^-] constitutes the electrophilic (negative) regions, the vicinity of imidazolium ring of the IL^- cation [$CnMIM^+$] forms the nucleophilic (positive) part and the alkyl chain of the IL^- cation [$CnMIM^+$] contributes to the neutral part (Figure 1b).

Table 2. Structural parameters of pristine α and β-PVDF and β-PVDF fragment of β-PVDF/IL complexes.

Structural parameters		Name of the molecule						
		α-PVDF with C_1 symmetry	β-PVDF with C_s symmetry	β-PVDF/ [C_2MIM] [BF_4]	β-PVDF/ [C_4MIM] [BF_4]	β-PVDF/ [C_6MIM] [BF_4]	β-PVDF/ [C_8MIM] [BF_4]	β-PVDF/ [C_{10}MIM] [BF_4]
Bond length (Å)	dC-F	1.38{1.34}	1.37 {1.34}	1.378	1.3777	1.3777	1.377	1.377
	dC-H	1.09{1.09}	1.09 {1.09}	1.0915	1.0914	1.0927	1.0914	1.0914
	dC-C	1.52{1.54}	1.53 {1.54}	1.522	1.522	1.522	1.522	1.522
Bond angle (°)	∠CF-CH-CF	116.4{116.5}	117.6 {112.5}	117.30	117.84	117.92	117.99	117.83
	∠CH-CF-CH	117.5 {118.5}	111.3 {112.5}	111.458	111.16	111.13	111.07	111.20
	∠F-C-F	105.8 {103}	106.9{108}	106.06	106.09	106.08	106.08	106.09
	∠H-C-H	108	108.8{112}	108.59	108.64	108.50	108.52	108.51
Dihedral angle (°)	C-C-C-C	171, 49{179,45}	180	168.05	172.86	173.50	173.80	173.58

experimental values are given within {} and taken from [20], parameter notations are in accordance with [18]

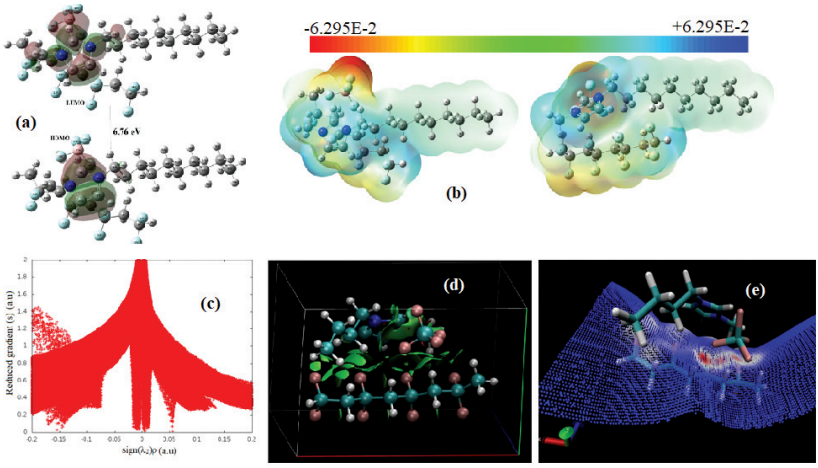

Figure 1. Plots for β-PVDF/[C10MIM][BF_4]: a) HOMO-LUMO plot, b) molecular electron static potential plot, mapped on to electron density, c) RDG plot, d) NCI isosurface plot, e) Hirshfeld surface plot, mapped on to electron density.

NBO analysis quantifies the loss of electron density (electron delocalization) from the donor (Lewis) NBOs into empty acceptor (non-Lewis) NBOs during interaction, resulting in significant departure from the idealized Lewis structures. The extent of electron delocalization is proportional to the stabilization energy ($E^{(2)}$) associated with i (donor) → j (acceptor) delocalization.

Total $E^{(2)}$ value corresponding to [BF_4]$^-$/β-PVDF interaction is found to be higher than [BMIM]$^+$/β-PVDF interaction (Table 3). Electron density (ρ) and Laplacian of electron density ($\nabla^2 \rho$) are obtained at the bond critical points(BCPs, where, $\nabla\rho = 0$) corresponding to relatively higher inter-unit NBO interaction regions, and given in Table 4. Positive values of $\nabla^2 \rho$and reasonably

small ρ values suggest presence of non-covalent interactions within the complex. Comparatively higher electron density values are found at the BCPs representing $[BF_4]^-$/β-PVDF interaction zones compared to $[BMIM]^+$/β-PVDF interaction zones (Table 5).

Table 3. Total energy differences of α-PVDF/[CnMIM][BF_4] and β-PVDF/[CnMIM][BF_4]; interaction energy, dipole moment and HOMO-LUMO energy gap for PVDF/IL complexes.

Ionic liquid (IL)	$E_{\alpha PVDF/IL}-E_{\beta PVDF/IL}$ (kJ/mol)	$\Delta E_{\alpha PVDF/IL}$ (kJmol)	$\Delta E_{\beta PVDF/IL}$ (kJ/mol)	$E_{LUMO}-E_{HOMO}$ for β-PVDF/IL (eV)	Dipole moment for	
					α-PVDF/IL (D)	β-PVDF/IL (D)
[C_2MIM][BF_4]	34	–43	–116	6.72	16.28	5.60
[C_4MIM][BF_4]	31	–47	–119	6.76	15.55	5.87
[C_6MIM][BF_4]	34	–48	–121	6.77	15.09	5.84
[C_8MIM][BF_4]	34	–48	–121	6.76	15.30	5.92
[C_{10}MIM][BF_4]	16	–66	–121	6.77	12.62	5.92

Table 4. $E^{(2)}$ corresponding to relatively higher NBO interactions.

$[BMIM]^+$/β-PVDF interactions					$[BF4]^-$/β-PVDF interactions				
Donor NBO	Type	Acceptor NBO	Type	$E^{(2)}$ (kcal/mol)	Donor NBO	Type	Acceptor NBO	Type	$E^{(2)}$ (kcal/mol)
LP F10	n	BD* C27-H37	σ*	0.33	LP F54	n	BD* C5-H23	σ*	2.41
LP F12	n	BD* C29-C30	π*	0.22	LP F54	n	BD* C3-H21	σ*	0.92
P F14	n	BD* C29-C30	π*	0.42	LP F55	n	BD* C1-H19	σ*	0.79
LP F16	n	BD* C34-H45	σ*	0.68	LP F55	n	BD* C3-H21	σ*	1.14
LP F16	n	BD* C36-H49	σ*	0.27					
BD C36-H50	σ	BD* C7-H25	σ*	0.48					
Total $E^{(2)}$				5.40	Total $E^{(2)}$				6.68

Table 5. Electron density (ρ) and Laplacian of electron density ($\nabla^2\rho$) at the BCPs corresponding to higher NBO interaction regions.

$[BMIM]^+$/β-PVDF interactions			$[BF4]^-$/β-PVDF interactions		
X – H⋯Y	ρ	$\nabla^2\rho$	X – H⋯Y	ρ	$\nabla^2\rho$
C27 – H37 ⋯ F10	0.00917	0.03702	C5 – H23 ⋯ F54	0.01520	0.05837
C29 = C30 ⋯ F14	0.00878	0.03582	C3 – H21 ⋯ F54	0.01138	0.04230
C34 – 45 ⋯ F16	0.00849	0.03094	C3 – H21 ⋯ F55	0.01189	0.04377
C36 – H49 ⋯ F16	0.00645	0.02307	C1 – H19 ⋯ F55	0.00813	0.02948

Reduced density gradient plot for β-PVDF/[BMIM][BF_4] is provided in Figure 1c. Prominent peaks appearing at the vicinity of zero electron density (at $\rho < 0.01$) in the RDG plot suggests weak inter-unit interaction of the system which is exactly in accordance with the three aforementioned approaches to analyse non-bonding interactions. NCI isosurface plot (Figure 1d) shows the inter-unit interaction regions as green isosurface (corresponding to weak van der Waals interaction) throughout the whole β-PVDF/[BMIM][BF_4] system. Inter-fragment Hirsfeld surface plot, mapped onto electron density values, also highlights that the regions with higher electron density (red coloured portions of the Hirshfeld surface, refer Figure 1e) are mostly situated at the $[BF_4]^-$/β-PVDF interaction zones.

Temperature dependence of standard statistical thermodynamic functions, e.g., specific heat at constant pressure (C_p^0), entropy (S^0) and enthalpy gradient [ddH = $H^0(T) - H^0(0)$] are obtained within the temperature range 100 K to 1000 K. All these parameters are found to increase with the increase in temperature which is resulted from the increase in molecular vibrational intensities with the increase in temperature.

A detailed density functional theory studies on PVDF/ionic liquid composite systems are provided in our recent paper [18].

4. Conclusions

Effects of ionic liquid addition on the structure and properties of PVDF polymer is demonstrated with the help of dispersion corrected density functional theory. IL molecules are found to exhibit better interaction with β-PVDF than α-PVDF, which explains the formation of β-PVDF crystal within α-PVDF blend as described in the experimental reports [3]. Reduction in dipole moment of β-PVDF/IL complex with respect to isolated β-PVDF infers better ion-dipolar interactions among β-PVDF and IL molecules. Variation in length of the alkyl chain attached to the imidazolium ring of the IL cation is found to have negligible effect on the PVDF/IL systems. Non-bonding interaction analyses suggest the presence of weak van der Waals interactions within the complexes. However, IL anion ($[BF_4]^-$)/β-PVDF interaction is found as relatively higher than IL cation ($[BMIM]^+$)/β-PVDF interaction. The uniqueness of this article is, it demonstrates the iner-fragment interactions within PVDF/IL clusters, for the first time, using quantum chemical approach. This article thoroughly explains how ionic liquids act as β-PVDF stabilizer, which is structurally unstable in the pristine phase. Moreover, it will be helpful to model similar kind of complex systems and to select the proper ionic liquid to synthesise electroactive β-PVDF from non-polar α-PVDF.

References

1. Itoh A., Takahashi Y., Furukawa T., Yajima H.: *Solid-state calculations of poly(vinylidene fluoride) using the hybrid DFT method: spontaneous polarization of polymorphs*, Polymer Journal, 2014, 46, 207–211.
2. Bohlé M., Bolton K.: *Conformational studies of poly(vinylidene fluoride), poly(trifluoroethylene) and poly(vinylidene fluoride-co-trifluoroethylene) using density functional theory*, Physical Chemistry Chemical Physics, 2014, 16, 12929–12939.
3. Mejri R., Dias J.C., Lopes A.C., Bebes Hentati S., Silva M.M., Botelho G., Mão de Ferro A., Esperança J.M.S.S., Maceiras A., Laza J.M., Vilas J.L., León L.M., Lanceros-Mendez S.: *Effect of anion type in the performance of ionic liquid/poly(vinylidene fluoride) electromechanical actuators*, European Polymer Journal, 2015, 71, 304–313.
4. Grimme S.: *Density functional theory with London dispersion correction*, WIREs Computational Molecular Science, 2011, 1, 211–228.
5. Clark T., Koch R.: *The chemist's electronic book of orbitals*, Springer-Verleg Heidelberg, New York, 1999.
6. Levine N.: *Quantum Chemistry, seventh ed.*, Pearson, New York, 2012.
7. Bader R.F.W.: *A bond path: a universal indicator of bonded interactions*, The Journal of Physical Chemistry, 1998, A102, 7314–7323.
8. Spackman M.A., Byrom P.G.: *A novel definition of a molecule in a crystal*, Chemical Physics Letters, 1997, 267, 215–220.
9. García C., Johnson E.R., Keinan S., Chaudret R., Piquemal J.P., Beratan D.N., Yang W.: *NCIPLOT: A program for plotting noncovalent interaction regions*, Journal of Chemical Theory and Computation, 2011, 7, 625–632.
10. Zhan C.G., Nichols J.A., Dixon D.A.: *Ionization potential, electron affinity, electronegativity, hardness, and electron excitation energy: Molecular properties from density functional theory orbital energies*, The Journal of Physical Chemistry A., 2003, 107(20), 4184–4195.
11. Elyukhin V.A.: *Statistical Thermodynamics of Semiconductor Alloys*, Elsevier, USA, 2016, 25–47.
12. Gaussian 09, Revision C.0, Gaussian:, Inc., Wallingford, CT, 2009.
13. Dennington R.D., Ketith T.A., Millam J.M., Gaussian Inc., 2008.
14. Lu T., Chen F.: *Multiwfn: A multifunctional wavefunction analyzer*, Journal of Computational Chemistry, 2012, 33, 580–592.

15. Humphrey W., Dalke A., Schulten K.: *VMD: Visual Molecular Dynamics*, Journal of Molecular Graphics and Modelling, 1996, 14, 33–38.
16. Irikura K.K.: *Thermo.pl*, National Institute of Standards and Technology, Gaithersburg, MD, 2002.
17. Weinholda F., Landisa C.R., Glendening E.D.: *What is NBO analysis and how is it useful?* International Review in Physical Chemistry, 2016, 35, 399–440.
18. Sarkar R., Kundu T.K.: *Density functional theory studies on PVDF/ionic liquid composite systems*, Journal of Chemical Sciences, 2018, 130, 115.
19. Wang Z.Y., Fan H.Q., Su K.H., Wen Z.Y.: *Structure and piezoelectric properties of poly(vinylidene fluoride) studied by density functional theory*, Polymer (Guildf), 2006, 47, 7988–7996.
20. Hasegawa R., Takahashi Y., Chatani Y., Tadokoro H.: *Crystal Structures of Three Crystalline Forms of Poly(vinylidene fluoride)*, Polymer Journal, 1971, 3, 600–610.